HHS Public Access

Author manuscript

J Pathol. Author manuscript; available in PMC 2019 October 01.

Published in final edited form as:

J Pathol. 2018 October ; 246(2): 231–243. doi:10.1002/path.5135.

Reduced RNA-binding protein HuD in pancreatic neuroendocrine tumors lowers p27^{Kip1} levels linked to poor prognosis

Chongtae Kim[1,†], **Da Eun Jeong**[2,†], **Sungeun Heo**[2], **Eunbyul Ji**[1], **Jun Gi Rho**[2], **Myeongwoo Jung**[1], **Sojin Ahn**[1], **Ye-Jin Kim**[2], **Yong-Sung Kim**[2], **Suk Woo Nam**[3], **Rohit N. Kulkarni**[4], **Kyoung Bun Lee**[5,*], **Eun Kyung Lee**[1,*], and **Wook Kim**[2,*]

[1]Department of Biochemistry, College of Medicine, The Catholic University of Korea, Seoul, South Korea

[2]Department of Molecular Science and Technology, Ajou University, Suwon, South Korea

[3]Department of Pathology, College of Medicine, The Catholic University of Korea, Seoul, South Korea

[4]Department of Islet Cell and Regenerative Biology, Joslin Diabetes Center and Department of Medicine, Harvard Medical School, and Harvard Stem Cell Institute, Boston, MA, USA

[5]Department of Pathology, Seoul National University College of Medicine, Seoul, South Korea

Abstract

For the majority of patients diagnosed with pancreatic neuroendocrine tumors (pancreatic NETs) there is a significant malignant potential with a poor prognosis, however the molecular abnormalities and pathogenesis of pancreatic NETs have not been firmly established. Here, we report that loss of RNA-binding protein HuD expression correlates with low p27^{Kip1} (p27) levels and poor prognosis in pancreatic NETs. HuD expression was frequently lost in many human pancreatic NETs and these pancreatic NETs showed aggressive clinico-pathological phenotypes with low p27 levels, increased tumor size, higher WHO grade and pathological T stage of the tumor, and presence of angioinvasion. Furthermore, loss of HuD was an independent, progress-free prognostic factor in multivariate survival analysis. However, level of HuR, the same Hu protein family member with HuD, was not significantly correlated with pancreatic NET size and progression. Mechanistically, HuD enhanced *p27* mRNA translation by interacting with both 5′- and 3′-untranslated regions (UTRs) of *p27* mRNA and consequently suppressed cell cycle progression and tumor growth. In addition, HuD competed with miR-30a-3p for binding to 3′UTR

[*]Correspondence to: Wook Kim, Department of Molecular Science and Technology, Ajou University, 206, World cup-ro, Yeongtong-gu, Suwon 16499, South Korea. wookkim21@ajou.ac.kr; Eun Kyung Lee, Department of Biochemistry, College of Medicine, The Catholic University of Korea, 222 Banpodae-ro, Seocho-gu, Seoul 06591, South Korea. leeek@catholic.ac.kr; or Kyoung Bun Lee, Department of Pathology, Seoul National University College of Medicine, 103 Daehak-ro, Jongno-gu, Seoul 03080, South Korea. azirang@gmail.com.

[†]Equal contributions.

Conflict of interest: The authors have declared that no conflict of interest exists.

Author contributions statement

K.B.L., E.K.L., and W.K. study concept and design; K.B.L., C.K., D.E.J., S.H., E.J., J.G.R., M.J., and S.A. acquisition of data; K.B.L., D.E.J., C.K., E.K.L., and W.K. analysis and interpretation of data; K.B.L., E.K.L., and W.K. drafting of the manuscript; Y.J.K., Y.S.K., S.W.N., and R.N.K. technical or material support; K.B.L., E.K.L., and W.K. study supervision. All authors gave final approval to the submitted and published versions.

of *p27* mRNA, suggesting interplay between HuD and miR-30a-3p in controlling p27 translation. Our results identify HuD as a pivotal suppressor of pancreatic NET growth, and propose that HuD has potential value as a prognostic factor of pancreatic NETs.

Keywords

RNA-binding protein; HuD; pancreatic neuroendocrine tumor; $p27^{Kip1}$; prognosis

Introduction

Pancreatic neuroendocrine tumors (pancreatic NETs), commonly referred to as “islet cell tumors”, are neuroendocrine tumors derived from the pancreatic endocrine cells present within the islets of Langerhans, and are classified into functional (such as insulinoma, the most prevalent functional pancreatic NET) and non-functional tumors, depending on whether or not they cause hormonal hypersecretion [1–3]. Most pancreatic NETs are indolent tumors but harbor a significant malignant potential; they are the second-most common malignancy of the pancreas, and patients with malignant pancreatic NETs have a short survival period [2–6]. In the past few decades, the incidence and prevalence of pancreatic NETs have increased substantially, although overall survival has remained relatively unchanged [2–5]. Further advances in our understanding of the cellular defects and molecular pathogenesis leading to pancreatic NETs could provide important answers that would lead to the identification of novel potential molecular targets and development of personalized and combination therapy to provide prolonged control or even cure the disease.

Cell cycle progression in mammals is driven by various complexes of cyclins and cyclin-dependent kinases (CDKs); the CDK inhibitory protein $p27^{Kip1}$ (p27, encoded by the gene *CDKN1B*) suppresses CDK activity and inhibits cell proliferation [7, 8]. Similar to that in other tumors, several studies have shown that loss of the tumor-suppressive function in p27 is one of the defects in pancreatic NETs and is associated with their high proliferation, poor prognosis, and shorter periods of overall survival [5, 6, 9–13]. This defective function of p27 results from its reduced expression and/or cytoplasmic mislocalization [13–18]. The overall abundance of p27 is regulated at the transcriptional, translational, and post-translational levels [7, 13–20]. However, many studies have demonstrated that during the cell cycle, oscillations in the abundance of p27 protein occurred without any changes in *p27* mRNA levels [7, 19–21]. The *p27* mRNA contains an internal ribosomal entry site (IRES) in the 5′-untranslated region (UTR) that is necessary for efficient p27 translation [20, 22]. Several RNA-binding proteins (RBPs) have been identified as specific binding factors of the IRES in the *p27* mRNA 5′-UTR and this binding regulates the IRES-dependent translation of *p27* mRNA [20, 22]. Further, in contrast to most tumor suppressors, gene mutation or silencing at the *CDKN1B* locus is rare [12, 19]. These observations indicate that the abundance of p27 is largely regulated by post-transcriptional mechanisms that include translational control [7, 19–22]. However, whether post-transcriptional regulation of *p27* mRNA contributes to the loss of p27 activity in pancreatic NETs, and which factor(s) are directly involved in this regulation, remain unknown.

Here, we identified human antigen D/embryonic lethal abnormal vision-like 4 (HuD/ELAVL4) as a key RBP that binds to the *p27* mRNA and enhances its translation in pancreatic NETs. Further, we provide evidence that loss of HuD is associated with increased tumor size and reduced time of survival in patients with pancreatic NETs. Four Hu/ELAVL family members have been identified; the largely neuronal members, HuB, HuC, and HuD, and the ubiquitous HuR [23]. Our previous study revealed that HuD was also expressed in pancreatic β cells [24]. Hu/ELAVL proteins bind to AU- and U-rich RNA elements in the 3′-UTR of target mRNAs and enhance their stability, thus indirectly increasing protein production [23, 25, 26]. Hu/ELAVL proteins can also modulate the translation of target mRNAs; unlike the effects on mRNA stability, they often serve as enhancers or repressors of translation [20, 22, 27]. Kullmann et al. showed that HuD and HuR binding to the *p27* 5′-UTR repress *p27* mRNA translation and promote cell cycle progression in non-neural/neuroendocrine cells [20]. Here, we report that unlike in the non-neural/neuroendocrine cells, HuD binds to both 5′- and 3′-UTRs of *p27* mRNA, and enhances p27 translation in pancreatic NET cells, leading to cell cycle arrest in the G1 phase. Accordingly, patients with HuD-negative pancreatic NETs had decreased p27 levels, increased tumor sizes, poor prognosis, and shorter progress-free survival time.

Materials and Methods

Patients

This study was approved by the International Review Board of Seoul National University Hospital (H-1602-034-739). We selected 88 patients who had been surgically treated for pancreatic NET, from 1994 to 2012, and obtained their medical records and formalin-fixed paraffin blocks of the tumor tissues from the archives of the department of pathology in Seoul National University Hospital (SNUH). The criterion of pathological T stage (pT) was based on the exocrine and endocrine pancreas tumor staging of the American Joint Committee on Cancer, 7th edition [28]. Criteria of WHO grade followed the 2017 new classification of neuroendocrine neoplasm [29]. Details are given in supplementary materials, Supplementary materials and methods.

Immunohistochemistry (IHC)

Paraffin sections were stained with primary antibodies against HuD, Ki-67, and p27, after an antigen retrieval process. Details for primary antibodies are listed in supplementary materials, Table S1. The slides were stained using an Ultravision LP kit (Lab Vision, Fremont, CA) or the Envision kit (DAKO, Glostrup, Denmark) and a Bond polymer Refine Detection kit (Leica, Wetzlar, Germany) and processed using a Bond-Max IHC and ISH slide stainer (Leica Biosystems, Wetzlar, Germany). Details of interpretation of IHC results are given in supplementary materials, Supplementary materials and methods. An H-score was calculated based on the intensity and percentage of positively stained cells, automatically counted by image analysis, and the following categories were assigned [30]. The intensity score (0 – 3+) was based on digitally measured intensity (range 0–240, black to white) and the range for each group was as follows; 0, 211–240; 1+, 189–210; 2+, 163–188; 3+, 0–162.

$$\text{H-score} = 3 \times (\%\ \text{at}\ 3+) + 2 \times (\%\ \text{at}\ 2+) + 1 \times (\%\ \text{at}\ 1+)\ (\text{range} = 0 - 300)\,.$$

Cell culture and transfection

Mouse insulinoma βTC6 cells were cultured in high-glucose DMEM (Invitrogen, Carlsbad, CA, USA) supplemented with 10% FBS (HyClone, Logan, UT, USA). βTC6 cell clones stably expressing Myc-HuD were obtained by transfection with pcDNA3.0-Myc-HuD, followed by selection for 2 wk in G418 (Invitrogen). βIRWT and βIRKO cells were established from wild-type (βIRWT) or β-specific insulin receptor-deficient (βIRKO) mice [24, 31–35]. βIRWT, βIRKO and Min6 cells were cultured in high-glucose DMEM (Invitrogen) supplemented with 10% FBS (HyClone, Logan, UT, USA). Details are given in supplementary materials, Supplementary materials and methods.

Biotin pull-down analysis

For *in vitro* synthesis of biotinylated transcripts, PCR fragments were prepared using 5′ primers that contained the T7 RNA polymerase promoter sequence (T7, CCAAGCTTCTAATACGACTCACTATAGGGAGA). Primer pairs used to synthesize DNA templates for the production of biotinylated transcripts spanning the *p27* mRNA (NM_009875.4) are listed in supplementary materials, Table S2. After purification of the PCR products, biotinylated transcripts were synthesized using MaxiScript T7 kit (Thermo Fisher Scientific, Waltham, MA, USA) and biotin-CTP (Enzo Life Sciences, Farmingdale, NY, USA). Biotin pull-down assays were performed by incubating whole-cell lysates (200 μg per sample) with 1 μg of purified biotinylated transcripts for 30 min at 25 °C, and then isolating the complexes with streptavidin-coupled Dynabeads (Invitrogen); the bound proteins present in the pull-down material were analyzed by Western blotting analysis [24, 36].

Statistical analyses

Quantitative data are presented as the mean ± SEM. Comparative analysis of HuD expression with clinicopathological parameters was assessed using a $\chi 2$ or Student's *t*-test. Survival analysis was performed using the Kaplan–Meier method and the Cox proportional hazard model. Differences between mean values in cell line experiments were compared statistically by Student's *t*-test. For analysis of time-course comparison between the groups in animal experiments, two-way ANOVA was performed followed by the Bonferroni *post hoc* test. All statistical analyses were performed using GraphPad Prism (GraphPad Software Inc, La Jolla, CA, USA) or the PASW statistics 18.0 software (SPSS, IBM, Armonk, NY, USA). A p value of < 0.05 was considered statistically significant.

Results

Loss of HuD expression in human pancreatic NET tissues is correlated with aggressive clinico-pathological phenotype

To investigate the expression patterns of HuD and p27 in human pancreatic NETs, we performed IHC for HuD and p27 in normal pancreas and tumors from patients ($n = 88$)

diagnosed with neuroendocrine tumors in pancreas. Consistent with our previous report [24], normal tissues showed positive staining of HuD in the endocrine islet cells and lack of staining in the exocrine tissue (Figure 1A; supplementary material, Figure S1). Similarly, p27 was expressed mainly in normal islet cells, with little, if any, expression in the exocrine tissue (Figure 1A). In contrast, we found considerable differences in immunoreactivity across the samples in the tumor cohort, ranging from negative to positive (Figure 1B; Table 1). The Positive expression rate of HuD in the 88 human pancreatic NETs was 73.9% (65/88 cases) and 26.1% (23/88 cases) were negative for HuD (Figure 1B; Table 1). Considering the positive expression of HuD in normal islet cells, its absence in 23 pancreatic NETs is most likely due to aberrant loss of the expression. As shown in Table 1, mitotic count and portion of G2 and G3 grade by 2017 WHO classification were higher in HuD (−) pancreatic NETs than HuD (+) pancreatic NETs. G2 and G3 pancreatic NETs are defined as well differentiated NET with different proliferative activity according to the 2017 WHO classification [29] and we excluded poorly differentiated neuroendocrine carcinoma (small cell carcinoma and neuroendocrine carcinoma). HuD (−) cases in this study showed the histologic features of NET that is trabecular, solid, or ribbon arrangement of round plump epithelial cells with salt and paper chromatin pattern and these histologic features were not different with HuD (+) cases. Other histologic features such as necrosis, plasmocytoid cell or tubular pattern, desmoplastic stroma and nuclear pleomorphism were also compared with HuD expression (supplementary material, Table S3). Plasmocytoid cells or tubular pattern was more frequently found in HuD (−) pancreatic NETs than HuD (+) pancreatic NETs, but necrosis, desmoplastic stroma and nuclear pleomorphism were not significantly different between HuD (+) and HuD (−) pancreatic NETs. In addition, we observed a positive relationship between HuD and p27 levels in human pancreatic NETs by IHC (Figure 1C). The expression of p27 was significantly decreased in HuD (−) pancreatic NETs compared with that in HuD (+) pancreatic NETs (H-score of p27 in HuD (−) versus HuD (+) pancreatic NETs=149.3±67.7 versus 209.0±58.3; $P < 0.001$) (Figure 1D; supplementary material, Table S4).

Next, we determined whether loss of HuD expression was related to pancreatic NET progression by analyzing the association between HuD and clinico-pathological status in pancreatic NETs. HuD (−) pancreatic NETs had higher Ki-67 index than HuD (+) pancreatic NETs (Figure 1E). Statistical analysis showed a strong correlation between HuD expression and tumor size ($P = 0.006$), grade based on the 2017 WHO classification ($P < 0.001$), mitotic counts ($P = 0.001$), invasion of other organs ($P = 0.003$), angioinvasion ($P = 0.033$), and pT stage ($P = 0.004$) (Figure 1F; Table 1). However, there was no significant difference in pN and pM stages between the two groups (Table 1). The rate of HuD (−) pancreatic NETs was higher in patients who had NET-associated syndromes such as Von-Hippel-Lindau (VHL) syndrome and multiple endocrine neoplasia (MEN) than in sporadic patients (Table 1). Notably, all pancreatic NET patients with MEN were negative for HuD expression. These associations were further confirmed by survival analysis, which suggested a positive correlation between tumoral HuD loss and a significantly reduced progress-free survival (PFS) rate (mean survival of HuD (−) versus HuD (+) patients, 70±11 versus 181±11 month; $P < 0.001$) (Figure 1G; Table 2). Furthermore, multivariate analysis using nine factors, which proved to have prognostic value in univariate survival analysis, showed that HuD

expression [Hazard ration (HR), 95% confidence interval (CI), 1.091–8.248; $P = 0.033$], sex (HR, 95% CI, 0.11–0.928; $P = 0.036$), tumor size (HR, 95% CI, 1.062–1.346; $P = 0.003$), and angioinvasion (HR, 95% CI, 1.025–8.886; $P = 0.045$) were independent prognostic factors for PFS in patients with pancreatic NET (Table 2).

As the ubiquitous RBP HuR is closely related and share several target mRNAs with HuD [23], we also evaluated whether HuR expression is correlated with tumor size, growth, and progression in the same pancreatic NET cohort. HuR was expressed in most area of normal pancreas including islet, acinar, and ductal cells (supplementary material, Figure S2). Although the differences in immunoreactivity for HuR across the samples was observed in the 88 human pancreatic NETs, only 6 samples (6.8%) were negative for HuR as well as its expression was not significantly correlated with pancreatic NET size, growth, and progression (supplementary material, Table S5).

HuD inhibits pancreatic NET cell proliferation, cell cycle progression, and tumor growth

Insulinoma, an islet cell tumor derived from pancreatic β cells, is one of the most common types of pancreatic NET, in which HuD is expressed [24] and p27 functions as the primary inhibitor of cell-cycle progression and proliferation [16, 37]. To investigate the biological significance of HuD expression in the development and progression of pancreatic NET, we performed gain-of-function and loss-of-function studies using Myc-HuD plasmid and HuD siRNA, respectively. We used a βTC6 cell line which stably overexpressed HuD (Myc-HuD) and a Min6 cell line with stably silenced HuD expression (shHuD). The expression of p27 protein in βTC6 cells decreased significantly by silencing HuD (Figure 2A) and increased by stable overexpression of Myc-HuD (supplementary material, Figure S3A). However, endogenous *p27* mRNA levels in βTC6 cells remained clearly unchanged after knockdown (Figure 2B) or stable overexpression of HuD (supplementary material, Figure S3B). By performing cell proliferation and colony forming assay, we found that silencing HuD increased the proliferative capacity of βTC6 cells as compared with that of cells containing control siRNA (Figure 2C, D). In contrast, HuD overexpression dramatically reduced the proliferative capacity of βTC6 cells (supplementary material, Figure S3C, D).

To gain insight into the mechanism by which HuD reduces pancreatic NET cell proliferation, we next analyzed differences in cell-cycle distributions by flow cytometry after HuD silencing or overexpression. Consistent with the changes in p27 levels after modulating HuD abundance, silencing HuD directed progression beyond the G1/S transition in βTC6 cells (Figure 2E), whereas G1/S arrest was observed in HuD-overexpressed βTC6 cells (supplementary material, Figure S3E). Similar effects were also observed in another insulinoma derived cell line, Min6, stably expressing control (shCtrl) or HuD shRNA (shHuD); p27 abundance was decreased and cell cycle progression was facilitated in shHuD cells compared with shCtrl cells (supplementary material, Figure S4A, B). Additionally, silencing HuD increased Ki-67-positive Min6 cells compared with control cells (supplementary material, Figure S4C). Collectively, these results show that HuD reduces cell proliferation by promoting p27 expression.

Since HuD represses *insulin* mRNA translation and decreases insulin production [24] and since insulin is a key growth factor that enhances pancreatic β-cell proliferation by

decreasing p27 levels [16, 31–35], we examined the potential role of insulin as a mediator of HuD-controlled p27 expression and pancreatic NET cell growth, using β cells derived from wild-type (βIRWT) or β-specific insulin receptor-deficient (βIRKO) mice [24, 31–35]. There were no significant differences in HuD-controlled p27 expression and cell-cycle progression between βIRWT and βIRKO cells (supplementary material, Figure S5A–C). These data suggest that HuD directly regulates p27 expression and cell cycle progression, independently of insulin signaling.

The effect of HuD on pancreatic NET cell growth was further confirmed by performing *in vivo* tumor growth assay. As the transplantation of insulinoma cells into normal mice causes death due to hypoglycemia, we transplanted βTC6 cells into BALB/c mice after a single intraperitoneal injection of streptozotocin (STZ; 200 mg/kg), which is a β cell toxin that produces a progressive increase in blood glucose levels over time as β cells die, and then either control or HuD siRNA was directly injected into xenograft tumors 3 times per week for one month (supplementary material, Figure S6A). There were no significant differences in body weight between control and HuD siRNA-injected mice (supplementary material, Figure S6B). HuD siRNA-injected tumors showed larger mean volumes, and formed more rapidly than control siRNA-injected tumors with decreased levels of HuD and p27 (Figure 2F; supplementary material, Figure S6C, D). Consistent with tumor growth data, blood glucose levels were significantly lower in HuD siRNA-injected group than in control siRNA-injected group (supplementary material, Figure S6E). Taken together, these data indicate that HuD inhibits pancreatic NET cell proliferation, *in vivo*.

HuD binds to both 5′- and 3′-UTRs of *p27* mRNA, and enhances its translation in pancreatic NET cells

To investigate the molecular mechanism by which HuD regulates p27 expression, we studied the interaction of HuD with the *p27* mRNAs by ribonucleoprotein immunoprecipitation analysis (RNP-IP) in βTC6 cells. The results showed enrichment of the *p27* mRNA in the HuD IP compared with the IgG IP (Figure 3A). To map a potential HuD binding region in the *p27* mRNA, biotinylated segments spanning the 5′-UTR (5U), coding region (CR), and 3′-UTR (3U-1 and 3U-2) were synthesized, and the RNP complexes of HuD and biotinylated RNAs were detected by biotin pull-down analysis using streptavidin-coated beads followed by Western blotting (Figure 3B). HuD interacted with both 5′- and 3′-UTRs of the *p27* mRNA, but not with the CR or a negative control transcript (spanning the 3′-UTR of *GAPDH* mRNA).

To determine whether the 5′- and 3′-UTRs are functional for the regulation of the *p27* mRNA by HuD, we generated reporter constructs derived from the vector pEGFP-N1 or -C1 in which the entire 5′-UTR (pEGFP-p27-5U) or 3′-UTR (pEGFP-p27-3U) was inserted before the translation start site or after the translation stop site of the EGFP coding region, respectively (Figure 3C). Each reporter construct was transfected into siRNA-transfected (siCtrl or siHuD) or plasmid-transfected (pcDNA or pHuD) βTC6 cells and EGFP expression was assessed by Western blot analysis. Consistent with the results in Figure 2A, silencing HuD selectively decreased EGFP expression in the pEGFP-p27-5U and pEGFP-p27-3U groups, but not in the control reporter group (pEGFP) (Figure 3D). Conversely, HuD

overexpression increased EGFP expression in the pEGFP-p27-5U and pEGFP-p27-3U groups, but not in the pEGFP group (Figure 3D). These data indicate that HuD can associate with the *p27* mRNA 5′- and 3′-UTRs, and that this association promotes p27 production.

To investigate whether HuD enhances translation of the *p27* mRNA, we carried out polysome analysis in Myc-HuD overexpressing βTC6 cells. Cytoplasmic extracts from control and HuD-overexpressing cells were fractionated through sucrose gradients, with the lightest components sedimenting at the top (fractions 1, 2), small (40S) and large (60S) ribosomal subunits and monosomes (80S) appearing in fractions 3–5, and progressively larger polysomes in fractions 6–12 (Figure 3E). Polysome-associated *p27* mRNA peaked in fraction 8 in vector-transfected cells, while overexpression of HuD increased the peak size of *p27* mRNA polysomes, which was highest in fraction 9 (Figure 3E). The distribution of the housekeeping *GAPDH* mRNA associated with polysomes largely overlapped between the two groups (Figure 3E). Additional evidence that HuD modulates p27 translation was obtained by nascent translation analysis. The incorporation of ^{35}S-Met and ^{35}S-Cys into newly synthesized p27 during a short time period (20 min) was decreased by HuD silencing and conversely, increased by HuD overexpression in the absence of changes in the reference protein GAPDH (Figure 3F). Collectively, these results strongly indicate that HuD increases p27 expression by enhancing the translation of *p27* mRNA.

miR-30a-3p represses p27 expression and competes with HuD for binding to *p27* 3′-UTRs

Using three different *in silico* analysis, we identified miR-30a-3p that can potentially target HuD binding site in the *p27* mRNA 3′-UTR (positions 2092–2212; p27-HuD BS) and regulate p27 expression. Indeed, ectopic expression of miR-30a-3p in βTC6 cells decreased the p27 expression, while inhibition of miR-30a-3p increased it (Figure 4A). Polysome analysis in βTC6 cells transiently transfected with miR-30a-3p showed that ectopic expression of miR-30a-3p reduced the association of *p27* mRNA with polysomes, suggesting a role of miRNA-30a-3p as repressor of p27 translation (Figure 4B). This was also supported by nascent translation analysis in βTC6 cells. Either ectopic expression of miR-30a-3p or silencing HuD decreased p27 translation, while ectopic expression of miR-30a-3p after transfection with siHuD further suppressed p27 translation (Figure 4C). As miR-30a-3p targets the p27-HuD BS, we sought to determine whether there is any interplay between HuD and miR-30a-3p in controlling p27 expression. RNP-IP analysis using an anti-HuD antibody and normal IgG in βTC6 cells transfected with pre- or anti-miR-30a-3p showed that enrichment of the *p27* mRNA in the HuD IP compared with the IgG IP was significantly reduced by pre-miR-30a-3p, but conversely, enhanced by anti-miR-30a-3p (Figure 4D). Accordingly, ectopic expression of miR-30a-3p in βTC6 cells transfected with siHuD elicited stronger suppression of p27 expression compared with that in βTC6 cells transfected with siCtrl (Figure 4E). To further confirm the functional interplay between HuD and miR-30a-3p in controlling p27 expression, we generated EGFP reporter constructs containing p27-HuD BS or a mutant p27-HuD BS (p27-HuD BS mut), which lack the seed region for base paring with miR-30a-3p, after the translation stop site of the EGFP coding region (Figure 4F). Silencing HuD decreased pEGFP-p27-HuD BS reporter expression, but did not affect the pEGFP-C1 control and pEGFP-p27-HuD BS mut reporter groups (Figure 4G). The pEGFP p27-HuD BS reporter expression was also regulated by miR-30a-3p;

ectopic expression of miR-30a-3p decreased the reporter expression, while inhibition of miR-30a-3p increased it (supplementary material, Figure S7). However, pEGFP-p27-HuD BS mut reporter expression was not affected by miR-30a-3p (Figure 4H). These results suggest that both HuD and miR-30a-3p bind to p27-HuD BS and regulate p27 expression. In addition, we followed the gain of function and loss of function experiments. Consistent with the results in Figure 4C–H, ectopic expression of HuD increased p27 expression in βTC6 cells, while miR-30a-3p decreased it (Figure 4E). However, the overexpression of miR-30a-3p along with HuD abolished the HuD-mediated up regulation of p27 expression (Figure 4I). This finding suggests that HuD and miR-30a-3p might compete for binding to p27-HuD BS.

Discussion

The majority of patients diagnosed with pancreatic NETs have tumors with a significant malignant potential and the prognosis of patients with progressive advanced pancreatic NETs is poor [1–6]. However, little is known about the molecular pathogenesis of pancreatic NETs; there is lack of good prognostic factors to stage disease extent, and the current effective treatments for pancreatic NETs are limited. There have been a number of recent advances that provide insights into molecular changes and the treatment of advanced pancreatic NETs, suggesting that therapeutic interventions targeting tumor-associated signaling pathways can be a future approach for pancreatic NETs [1, 38–41]. Treatment with the multi-target tyrosine kinase inhibitor sunitinib and the oral mTOR inhibitor everolimus significantly improved progression-free survival compared to placebo among patients with advanced pancreatic NETs [39, 41]. In addition, targeting β-catenin signaling can suppress the tumorigenesis and growth of pancreatic NETs and significantly prolongs the survival rate in mice [38]. These findings highlight an imperative need for identification of new potential molecular targets and the development of therapeutic agents. Thus, a great challenge lies ahead in understanding the molecular mechanisms leading to the development of pancreatic NETs and further advances in our understanding of the cellular defects and the molecular pathogenesis should contribute to identifying novel prognostic molecular markers that can facilitate the development of appropriate therapeutic strategies.

We provide evidence that pancreatic NETs with loss of HuD expression show aggressive clinicopathological phenotype. HuD expression is closely associated with tumor size and tumor stage and can be potentially correlated with pancreatic NET progression. Moreover, HuD loss proved to be an independent, progress-free predictor of pancreatic NETs, along with tumor size and angioinvasion, to affect prognosis in multivariate analysis. Notably, there is a positive correlation between the tumoral HuD loss and a significantly reduced PFS rate. The results of our study also showed the pathological and tumor-suppressive roles of HuD in inhibiting cell proliferation and cell cycle progression. Thus, our results identify HuD as a tumor suppressor in pancreatic NETs and suggest that it may be a valuable prognostic factor and therapeutic target for pancreatic NETs.

p27 functions as the primary inhibitor of cell cycle progression and proliferation in the pancreatic endocrine cells, especially pancreatic β cells [16, 37], as well as attenuated expression of p27 in MENs is associated with a malignant pancreatic NETs [5, 6, 9],

implying that loss of p27 might be one of the defects present in benign and malignant pancreatic NETs. These data are in line with results from HuD (−) pancreatic NETs, which show significantly decreased p27 expression and increased proliferative capacity, leading to increased tumor size, poor prognosis, and shorter PFS time. In agreement with these results, HuD silencing in pancreatic NET cell lines decreased *p27* mRNA translation by direct interaction with *p27* mRNA, resulting in decreased p27 levels. As a result, suppressing HuD could facilitate cell-cycle progression and the tumorigenesis and growth of pancreatic NETs. Moreover, a positive correlation between HuD and p27 expression was observed in clinical pancreatic NET tissues, further supporting the role of HuD in maintaining p27 abundance and thereby exerting tumor-suppressive effects. In addition, we also found that HuD binds to the 3′-UTR of *p27* mRNA and competes with miR-30a-3p for binding to this site. miR-30a-3p decreased p27 expression as well as inhibited HuD-mediated p27 expression, likely due to competition with HuD for the binding to mRNA. These results suggest an interplay between HuD and miR-30a-3p in controlling p27 expression.

In contrast to our findings that HuD enhances *p27* mRNA translation and induce cell-cycle arrest at G1 phase in pancreatic NET cell lines, Kullmann et al. proposed that HuD represses *p27* mRNA translation, and promotes cell-cycle progression in non-neural/neuroendocrine cells including HeLa and 293T cells [20]. However, HuD expression is restricted to neural/neuroendocrine cells and HuD is not present in these non-neural/neuroendocrine cells. In addition, although HuR and HuD are closely related and share several target mRNAs, it is unlikely that they always have same outputs in the same cells or target molecules. For example, HuD, but not HuR, induced a neurite outgrowth in PC12 cells [42]. Based on our unpublished results not shown in this study, HuD induced p27 expression in human neuroblastoma SH-SY5Y cells, similar to the results presented in this study. However, HuR repressed p27 expression in these cells as well as in other non-neural/neuroendocrine cells including Hep3B, HeLa, HCT116, and MCF7 cells, which is consistent with the previous report [20]. Accordingly, HuR expression was not significantly correlated with pancreatic NET size and progression. In addition, HuD competes with the microRNA miR-196b for binding to the same site in the 5′-UTR of preproinsulin (*Ins2*) mRNA to regulate *Ins2* mRNA translation [24, 43], whereas HuR did not associate with *Ins2* mRNA [24]. These results suggest that they do not always share the same target mRNAs and that the difference in effects would be due to the interaction with different counterparts.

In addition to neuronal cells, HuD has been found to be expressed in many neuroendocrine cells, including pancreatic islet cells such as α and β cells [24]. Our study shows that HuD expression is lost in many human pancreatic NETs (26.1%) and these pancreatic NETs show aggressive clinico-pathological phenotypes with increased tumor size, poor prognosis, and shorter PFS time in a p27-dependent manner, suggesting that high expression of HuD might be a suitable biomarker of good prognosis. Although the underlying molecular defects related to HuD loss were not elucidated, these findings pave the way to the understanding of the molecular mechanism leading to pancreatic NETs and, hence the identification of new potential molecular targets.

Supplementary Material

Refer to Web version on PubMed Central for supplementary material.

Acknowledgments

We thank Hyun-Jin Tae of Chonbuk National University for technical support. This work was supported by Basic Science Research Program through the National Research Foundation of Korea (NRF) funded by the Ministry of Science, ICT & Future (2016R1E1A1A01941213, 2014R1A2A1A11053431 and 2012M3A9D1054517). R.N.K. acknowledges support from National Institutes of Health Grant R01 DK67536 and R01 DK103215.

References

1. Metz DC, Jensen RT. Gastrointestinal Neuroendocrine Tumors: Pancreatic Endocrine Tumors. Gastroenterology. 2008; 135:1469–1492. [PubMed: 18703061]
2. Ramage JK, Ahmed A, Ardill J, et al. Guidelines for the management of gastroenteropancreatic neuroendocrine (including carcinoid) tumours (NETs). Gut. 2012; 61:6–32. [PubMed: 22052063]
3. Yao JC, Hassan M, Phan A, et al. One hundred years after “carcinoid”: epidemiology of and prognostic factors for neuroendocrine tumors in 35,825 cases in the United States. J Clin Oncol. 2008; 26:3063–3072. [PubMed: 18565894]
4. Halfdanarson TR, Rabe KG, Rubin J, et al. Pancreatic neuroendocrine tumors (PNETs): incidence, prognosis and recent trend toward improved survival. Ann Oncol. 2008; 19:1727–1733. [PubMed: 18515795]
5. Zhang J, Francois R, Iyer R, et al. Current understanding of the molecular biology of pancreatic neuroendocrine tumors. J Natl Cancer Inst. 2013; 105:1005–1017. [PubMed: 23840053]
6. Ishida E, Yamada M, Horiguchi K, et al. Attenuated expression of menin and p27 (Kip1) in an aggressive case of multiple endocrine neoplasia type 1 (MEN1) associated with an atypical prolactinoma and a malignant pancreatic endocrine tumor. Endocr J. 2011; 58:287–296. [PubMed: 21441703]
7. Hengst L, Reed SI. Translational control of p27Kip1 accumulation during the cell cycle. Science. 1996; 271:1861–1864. [PubMed: 8596954]
8. Sherr CJ, Roberts JM. CDK inhibitors: positive and negative regulators of G1-phase progression. Genes Dev. 1999; 13:1501–1512. [PubMed: 10385618]
9. Wu T, Hua X. Menin represses tumorigenesis via repressing cell proliferation. Am J Cancer Res. 2011; 1:726–739. [PubMed: 22016823]
10. Grabowski P, Schrader J, Wagner J, et al. Loss of nuclear p27 expression and its prognostic role in relation to cyclin E and p53 mutation in gastroenteropancreatic neuroendocrine tumors. Clin Cancer Res. 2008; 14:7378–7384. [PubMed: 19010853]
11. Kim HS, Lee HS, Nam KH, et al. p27 loss is associated with poor prognosis in gastroenteropancreatic neuroendocrine tumors. Cancer Res Treat. 2014; 46:383–392. [PubMed: 25036575]
12. Marinoni I, Pellegata NS. p27kip1: a new multiple endocrine neoplasia gene? Neuroendocrinology. 2011; 93:19–28. [PubMed: 20980721]
13. Karnik SK, Hughes CM, Gu X, et al. Menin regulates pancreatic islet growth by promoting histone methylation and expression of genes encoding p27Kip1 and p18INK4c. Proc Natl Acad Sci USA. 2005; 102:14659–14664. [PubMed: 16195383]
14. Karnik SK, Chen H, McLean GW, et al. Menin controls growth of pancreatic beta-cells in pregnant mice and promotes gestational diabetes mellitus. Science. 2007; 318:806–809. [PubMed: 17975067]
15. Medema RH, Kops GJ, Bos JL, et al. AFX-like Forkhead transcription factors mediate cell-cycle regulation by Ras and PKB through p27kip1. Nature. 2000; 404:782–787. [PubMed: 10783894]
16. Uchida T, Nakamura T, Hashimoto N, et al. Deletion of Cdkn1b ameliorates hyperglycemia by maintaining compensatory hyperinsulinemia in diabetic mice. Nat Med. 2005; 11:175–182. [PubMed: 15685168]

17. Viglietto G, Motti ML, Bruni P, et al. Cytoplasmic relocalization and inhibition of the cyclin-dependent kinase inhibitor p27(Kip1) by PKB/Akt-mediated phosphorylation in breast cancer. Nat Med. 2002; 8:1136–1144. [PubMed: 12244303]
18. Wander SA, Zhao D, Slingerland JM. p27: a barometer of signaling deregulation and potential predictor of response to targeted therapies. Clin Cancer Res. 2011; 17:12–18. [PubMed: 20966355]
19. Koff A. How to decrease p27Kip1 levels during tumor development. Cancer Cell. 2006; 9:75–76. [PubMed: 16473274]
20. Kullmann M, Göpfert U, Siewe B, et al. ELAV/Hu proteins inhibit p27 translation via an IRES element in the p27 5′UTR. Genes Dev. 2002; 16:3087–3099. [PubMed: 12464637]
21. Agrawal D, Hauser P, McPherson F, et al. Repression of p27kip1 synthesis by platelet-derived growth factor in BALB/c 3T3 cells. Mol Cell Biol. 1996; 16:4327–4336. [PubMed: 8754833]
22. Millard SS, Vidal A, Markus M, et al. A U-rich element in the 5′ untranslated region is necessary for the translation of p27 mRNA. Mol Cell Biol. 2000; 20:5947–5959. [PubMed: 10913178]
23. Hinman MN, Lou H. Diverse molecular functions of Hu proteins. Cell Mol Life Sci. 2008; 65:3168–3181. [PubMed: 18581050]
24. Lee EK, Kim W, Tominaga K, et al. RNA-binding protein HuD controls insulin translation. Mol Cell. 2012; 45:826–835. [PubMed: 22387028]
25. Beckel-Mitchener AC, Miera A, Keller R, et al. Poly(A) tail length-dependent stabilization of GAP-43 mRNA by the RNA-binding protein HuD. J Biol Chem. 2002; 277:27996–28002. [PubMed: 12034726]
26. Yano M, Okano HJ, Okano H. Involvement of Hu and hnRNP K in neuronal differentiation through p21 mRNA post-transcriptional regulation. J Biol Chem. 2005; 280:12690–12699. [PubMed: 15671036]
27. Ratti A, Fallini C, Colombrita C, et al. Post-transcriptional Regulation of Neuro-oncological Ventral Antigen 1 by the Neuronal RNA-binding Proteins ELAV. J Biol Chem. 2008; 283:7531–7541. [PubMed: 18218628]
28. American Joint committee on cancer. Exocrine and endocrine pancreas. In: Edge S, Byrd DR, Compton CC, Fritz AG, Greene FL, Trotti A, editorsAJCC Cancer staging Manual. 7. New York: Springer; 2010. 241–249.
29. Rindi G, Arnoid R, Bisman F, Capell C, Klimstra D, Koppep G. WHO classification of tumours of the digestive system. 4. International Agency for Research on Cancer; Lyon: 2017. 210–214.
30. Pierceall WE, Wolfe M, Suschak J, et al. Strategies for H-score normalization of preanalytical technical variables with potential utility to immunohistochemical-based biomarker quantitation in therapeutic response diagnostics. Anal Cell Pathol. 2011; 34:159–168.
31. Assmann A, Ueki K, Winnay JN, et al. Glucose effects on beta-cell growth and survival require activation of insulin receptors and insulin receptor substrate 2. Mol Cell Biol. 2009; 29:3219–3228. [PubMed: 19273608]
32. Kim W, Doyle ME, Liu Z, et al. Cannabinoids inhibit insulin receptor signaling in pancreatic β cells. Diabetes. 2011; 60:1198–1209. [PubMed: 21346174]
33. Kim W, Lao Q, Shin YK, et al. Cannabinoids induce pancreatic β-cell death by directly inhibiting insulin receptor activation. Sci Signal. 2012; 5:ra23. [PubMed: 22434934]
34. Kulkarni RN, Brüning JC, Winnay JN, et al. Tissue-specific knockout of the insulin receptor in pancreatic beta cells creates an insulin secretory defect similar to that in type 2 diabetes. Cell. 1999; 96:329–339. [PubMed: 10025399]
35. Kulkarni RN, Winnay JN, Daniels M, et al. Altered function of insulin receptor substrate-1-deficient mouse islets and cultured beta-cell lines. J Clin Invest. 1999; 104:R69–R75. [PubMed: 10606633]
36. Kim C, Kim W, Lee H, et al. The RNA-binding protein HuD regulates autophagosome formation in pancreatic β cells by promoting autophagy-related gene 5 expression. J Biol Chem. 2014; 289:112–121. [PubMed: 24275661]
37. Georgia S, Bhushan A. p27 regulates the transition of beta-cells from quiescence to proliferation. Diabetes. 2006; 55:2950–2956. [PubMed: 17065330]

38. Jiang X, Cao Y, Li F, et al. Targeting β-catenin signaling for therapeutic intervention in MEN1-deficient pancreatic neuroendocrine tumours. Nat Commun. 2014; 5:5809. [PubMed: 25517963]
39. Raymond E, Dahan L, Bang YJ, et al. Sunitinib malate for the treatment of pancreatic neuroendocrine tumours. N Engl J Med. 2011; 364:501–513. [PubMed: 21306237]
40. Ro C, Chai W, Yu VE, et al. Pancreatic neuroendocrine tumors: biology, diagnosis, and treatment. Chin J Cancer. 2013; 32:312–324. [PubMed: 23237225]
41. Yao JC, Shah MH, Ito T, et al. Everolimus for advanced pancreatic neuroendocrine tumors. N Engl J Med. 2011; 364:514–523. [PubMed: 21306238]
42. Brennan CM, Steitz JA. HuR and mRNA stability. Cell Mol Life Sci. 2001; 58:266–277. [PubMed: 11289308]
43. Panda AC, Sahu I, Kulkarni SD, et al. miR-196b-mediated translation regulation of mouse insulin2 via the 5′UTR. PLoS One. 2014; 9:e101084. [PubMed: 25003985]

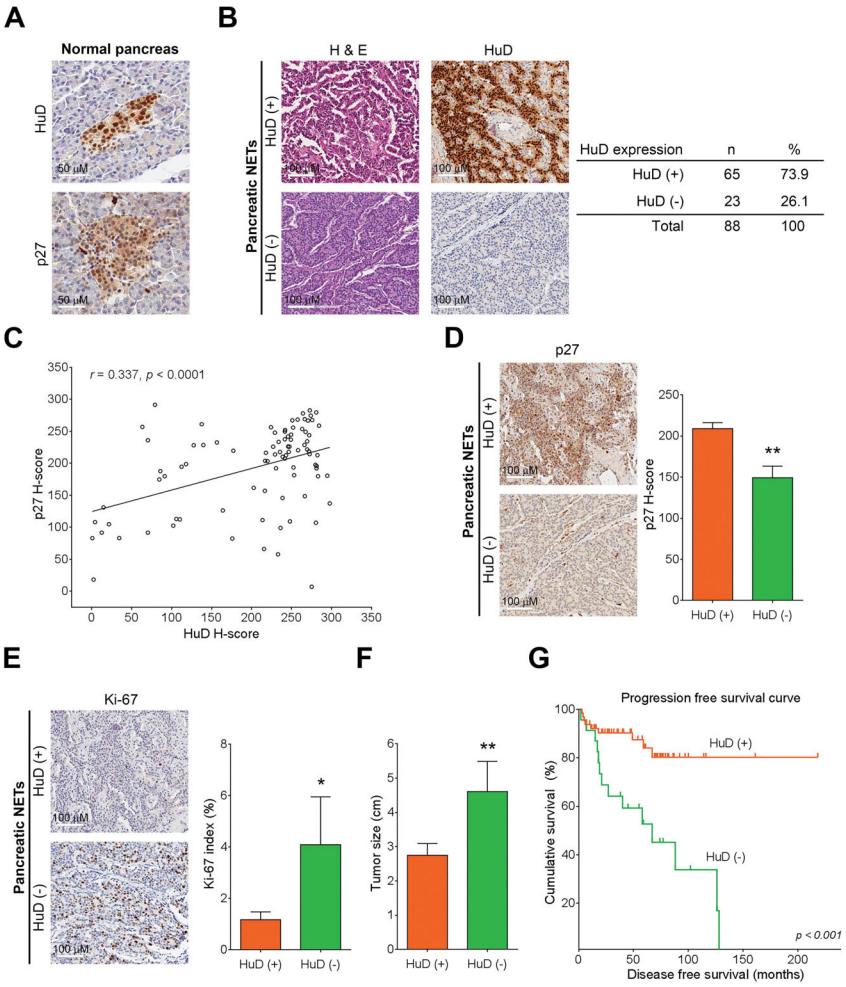

Figure 1.

Loss of HuD is associated with increased tumor size and shorter progression free survival times in patients with pancreatic NET. (A) HuD and p27 expression in human pancreatic islets (IHC, ×400). (B) Representative images (H&E and IHC, ×200) of HuD positive (+) and negative (−) expression in human pancreatic NET tissues. HuD (+) and HuD (−) pancreatic NETs are G1 grade (Ki-67 index 0.72%, mitotic activity 0/10HPF) and G2 grade (Ki-67 index 27.06%, mitotic activity 43/10HPF), respectively. Quantification for HuD staining is shown on the right. (C) Positive correlation between p27 and HuD H-scores was detected in 88 samples of human pancreatic NETs (r = 0.337; $P < 0.0001$). (D) Representative IHC images of positive p27 expression in G1 grade HuD (+) pancreatic NETs and negative p27 expression in G2 grade HuD (−) pancreatic NETs (×200). Quantification of p27 H-score in HuD (+) and (−) pancreatic NETs is shown on the right. (E) Representative IHC images of Ki-67 expression in G1 grade HuD (+) and G2 grade HuD (−) pancreatic NET tissues (×200). Quantification of Ki-67 index in HuD (+) and (−) pancreatic NETs is shown on the right. (F) Quantification of tumor size in HuD (+) and (−) pancreatic NETs. All data (B–F) are shown as the mean ± SEM (n = 88). *$P < 0.05$, **$P < 0.01$. (G) Progression free survival curves of HuD (+) and (−) pancreatic NET patients (n = 88). $P < 0.001$.

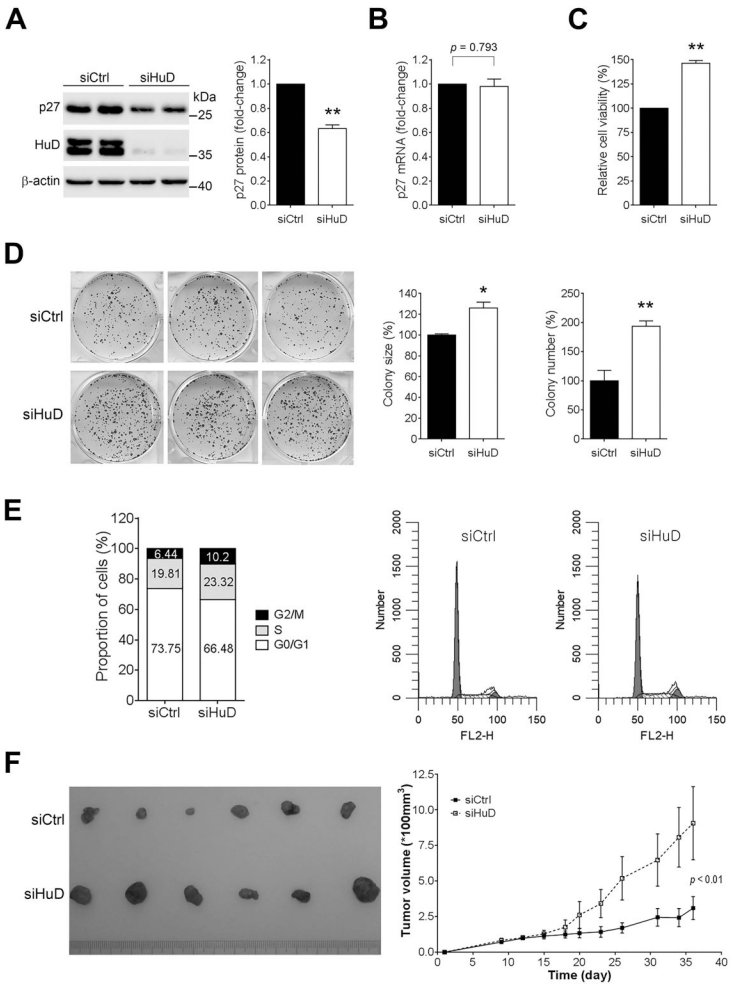

Figure 2.

HuD increases p27 expression and inhibits pancreatic NET cell growth. (A) The levels of p27 in βTC6 cells transiently transfected with siRNAs were assessed by Western blot analysis. Relative density for p27 proteins is shown on the right. (B) The levels of *p27* mRNA in βTC6 cells transiently transfected with siRNAs were quantified by RT-qPCR analysis. All mRNA amounts were normalized to the levels of *18S* rRNA. $P = 0.793$. (C) Cell viability was determined by MTS assay 48 h after transfection with the indicated siRNAs into βTC6 cells. (D) Colony formation assay in βTC6 cells transfected with the indicated siRNAs. Colonies were stained with crystal violet and the number and size of colonies were analyzed. Quantification of colony size and number is shown on the right. All data (A–D) are shown as the mean ± SEM ($n = 3$). *$P < 0.05$, **$P < 0.01$. (E) Flow cytometric analysis in βTC6 cells transfected with the indicated siRNAs. (F) Effects of HuD knockdown on tumor growth in vivo. *Left*: Images of tumors formed in nude mice injected subcutaneously with the HuD-silencing βTC6 cells. *Right*: Tumor growth curves. ($n = 6$ for each group; mean ± SEM). $P < 0.01$ by two-way ANOVA with the Bonferroni post hoc test.

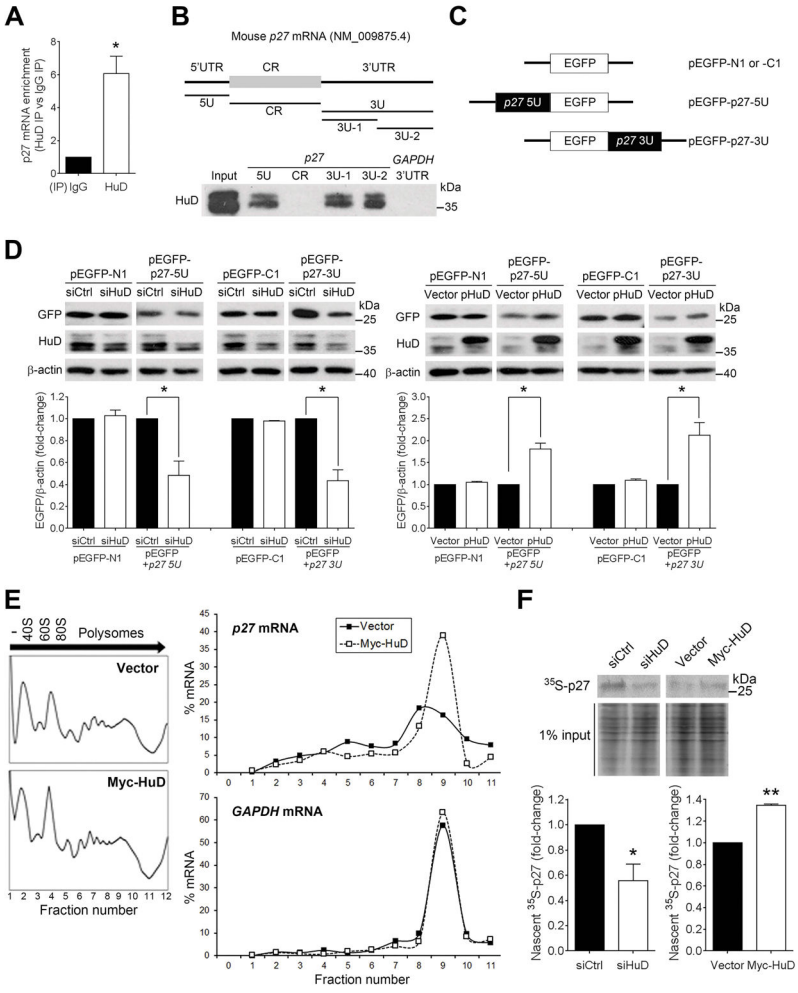

Figure 3.

HuD binds to the *p27* 5′- and 3′-UTRs and enhances p27 translation. (A) βTC6 cell lysates were subjected to RNP-IP followed by RT-qPCR analysis to measure the enrichment of *p27* mRNA in HuD IP compared with control IgG IP. All mRNA amounts were normalized to the levels of *18S* rRNA. (B) *Top*, schematic representation of the mouse *p27* mRNA and biotinylated segments (5U, CR, 3U) and sub-fragments of the 3′-UTR (3U-1 and 3U-2) synthesized for analysis. *Bottom*, biotin pull-down analysis to assess the interaction of HuD and the biotinylated RNAs shown in the top. Biotinylated *GAPDH* 3′-UTR was included as negative control. (C) Schematic representation of reporter plasmids: parent vector (pEGFP-N1 or -C1), a plasmid expressing only one copy of fragment *p27* 5′-UTR (pEGFP-p27-5U) and a plasmid expressing only one copy of fragment *p27* 3′-UTR (pEGFP-p27-3U). (D) 48 h after transfection of either siCtrl or siHuD or 24 h after transfection with either control plasmid (vector) or a plasmid expressing HuD (pHuD), together with each reporter plasmids, the levels of EGFP, HuD, and loading control were assessed by Western blot analysis. After quantification by densitometry, EGFP signals were expressed relative to EGFP levels in the siCtrl or vector sample in each pair. (E) Polysome analysis of *p27* mRNA. Lysates from βTC6 cells transfected with either vector or pHuD were fractionated through sucrose gradients to generate polysome profiles (*left*). Arrow: direction of sedimentation; –, no

ribosomal components; small (40S) and large (60S) ribosome subunits; 80S, monosomes; low- and high-molecular weight polysomes (polysomes, fractions 6–11), respectively. The relative distribution of *p27* mRNA and housekeeping *GAPDH* mRNA on polysome gradients was studied by RT-qPCR analysis of the RNA present in each of 11 gradient fractions, and represented as % of total mRNA (*right*). Data are representative of three independent experiments. (F) Nascent translation of p27 was monitored by incubation of βTC6 cells for 20 min in the presence of ^{35}S-Met/Cys. After IP using anti-p27 antibody, the newly translated proteins were visualized by SDS-PAGE, transfer, and PharoseFX Plus. Quantification of ^{35}S-p27 is shown at the bottom. All data (A, D, and F) are shown as the mean ± SEM ($n = 3$). *$P < 0.05$, **$P < 0.01$.

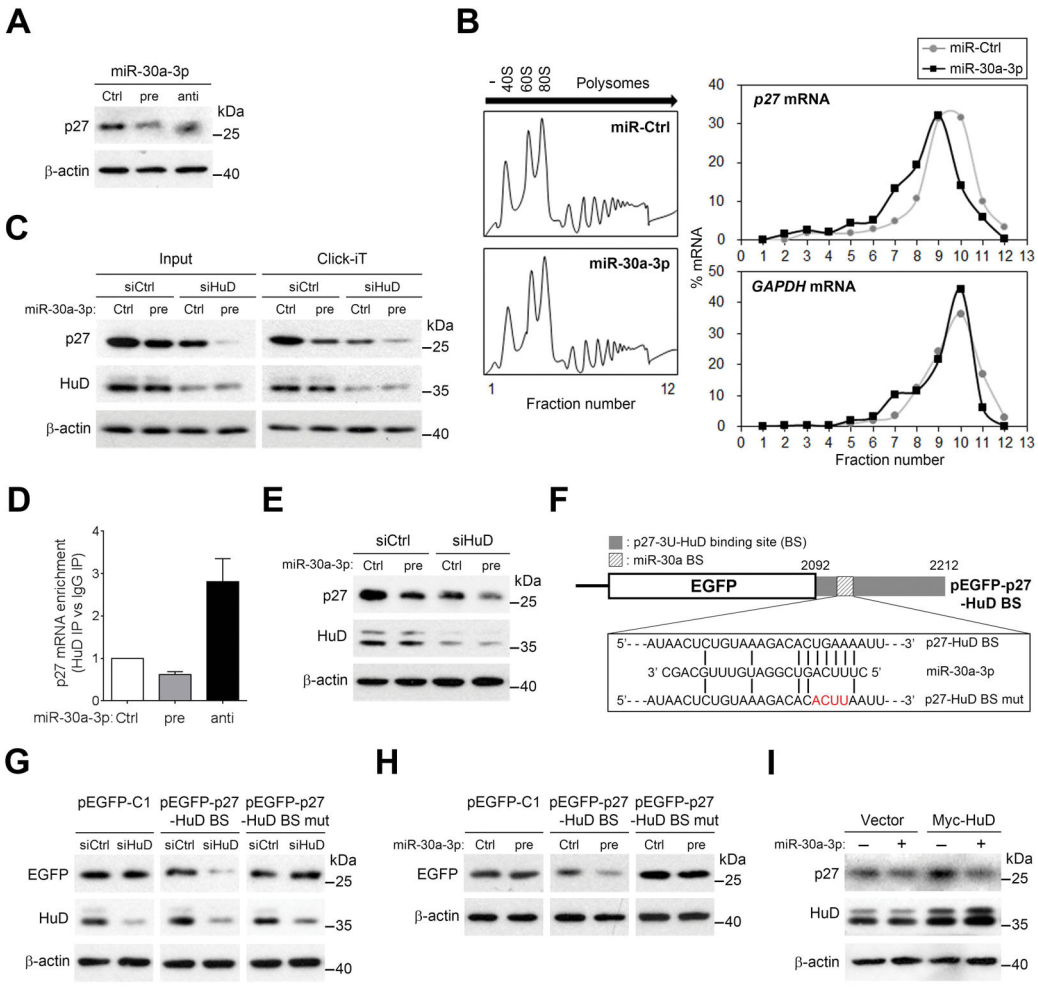

Figure 4.

Ectopic expression of miR-30a-3p along with HuD abolished the HuD-mediated up regulation of p27 expression. (A) miR-30a-3p represses p27 expression. After transfection with Ctrl, pre-miR-30a-3p, and anti-miR-30a-3p for 48 h, p27 protein levels were assessed by Western blotting. (B) Polysome analysis of *p27* mRNA in βTC6 cells transfected with either Ctrl or pre-miR-30a-3p. The relative distribution of *p27* mRNA and reference *GAPDH* mRNA on polysome gradients was assessed by RT-qPCR analysis of the RNA present in each of 12 gradient fractions, and represented as % of total mRNA (*right*). (C) Nascent translation of p27 in βTC6 cells transfected with control (siCtrl) or HuD (siHuD) siRNA along with pre-miR-30a-3p. The *de novo* protein synthesis were assessed by Click-iT assay. (D) RNP-IP followed by RT-qPCR analysis to measure the enrichment of *p27* mRNA in HuD IP compared with control IgG IP in βTC6 cells transfected with Ctrl, pre-miR-30a-3p, and anti-miR-30a-3p. All mRNA amounts were normalized to the levels of *18S* rRNA. (E) Western blotting for p27 in βTC6 cells transfected with siCtrl or siHuD along with pre-miR-30a-3p. (F) Schematic representation of the pEGFP-p27-HuD binding site (BS) reporter constructs. A wildtype p27-HuD BS was inserted into pEGFP-C1; a mutant reporter construct (p27-HuD BS mut) lacking the seed region for base paring with miR-30a-3p was generated using site-directed mutagenesis. The vertical lines between the

sequences denote base pairing. (G) Reporter analysis in βTC6 cells transfected with siCtrl or siHuD. After transfection with pEGFP-C1 control vector, pEGFP-p27-HuD BS or pEGFP-p27-HuD BS mut reporter construct along with siCtrl or siHuD, the levels of EGFP, HuD, and loading control were assessed by Western blotting. (H) Reporter analysis in βTC6 cells transfected with Ctrl or pre-miR-30a-3p. After transfection with pEGFP-C1 control vector, pEGFP-p27-HuD BS or pEGFP-p27-HuD BS mut reporter construct along with Ctrl or pre-miR-30a-3p, the levels of EGFP and loading control were assessed by Western blotting. (I) HuD-mediated p27 expression is suppressed by miR-30a-3p. After transfection with Ctrl or miR-30a-3p, βTC6 cells were transfected with pcDNA (Vector) or pcDNA-Myc-HuD (Myc-HuD) and then the levels of p27, HuD, and loading control were assessed by Western blotting.

Table 1

Correlation between HuD expression and pancreatic NET clinico-pathological features of 88 patients

		HuD		
	n	**Negative (*n* = 23)**	**Positive (*n* = 65)**	***P* value**
Sex				
male	43	13 (56.5%)	20 (46.2%)	0.393
female	45	10 (43.5%)	35 (53.8%)	
Age (year)[a]	54	53.4±13.5	52.3±11.4	0.488
Size (cm)[a]	2.4	4.6±4.2	2.7±2.8	0.006**
Grade by 2017 WHO classification				
G1	64	11 (47.8%)	53 (81.5%)	< 0.001**
G2	20	8 (34.8%)	12 (18.5%)	
G3	4	4 (17.4%)	0 (0.0%)	
Mitotic count (10HPF) [a]		5.9±10.9	0.7±2.1	0.001**
Extent of invasion				
Limited in pancreas	63	11 (47.8%)	52 (80.0%)	0.003**
Extended to other organ	25	12 (52.2%)	13 (20.0%)	
Angioinvasion				
Absent	58	11 (47.8%)	47 (72.3%)	0.033*
Present	30	12 (52.2%)	18 (27.7%)	
pT (AJCC 7th ed)				
1	32	3 (13.0%)	29 (44.6%)	0.004**
2	31	8 (34.8%)	23 (35.4%)	
3	25	12 (52.2%)	13 (20.0%)	
pN				
0	80	21 (26.3%)	59 (90.8%)	0.98
1	8	2 (8.7%)	6 (9.2%)	
pM				
0	81	21 (91.3%)	60 (92.3%)	1.000
1	7	2 (8.7%)	5 (7.7%)	
Associated syndrome				
Sporadic	80	18 (78.3%)	62 (95.4%)	0.009**
Von-Hippel-Lindau syndrome (VHL)	5	2 (8.7%)	3 (4.6%)	
Multiple endocrine neoplasm (MEN)	3	3 (13.0%)	0 (0.0%)	

[a] mean±SD,

* $P < 0.05$,

** $P < 0.01$

Table 2

Correlation between HuD expression and progression-free survival in 88 pancreatic NET patients

		Univariate analysis			Multivariate analysis		
	n	**Progression (%)**	**Mean ± SE (month)**	***P* value**	**Hazard ratio (95% CI)**		***P* value**
HuD							
Negative	23	14 (60.9)	70±11	< 0.001**	3.506	[1.246–9.871]	0.018*
Positive	65	9 (13.8)	181±11		1		
Sex							
male	43	14 (32.6)	134±18	0.042*	1		
female	45	9 (20.0)	114±10		0.28	[0.095–0.827]	0.021*
Age (year)[a]		0.998	[0.962–1.036]	0.931			
Size (cm)[a]		1.3	[1.178–1.431]	< 0.001**	1.209	[1.071–1.385]	0.002**
Grade by 2017 WHO classification							
G1	64	12 (18.7)	158±17	0.001**			
G2	20	7 (35.0)	88±14				
G3	4	4 (100.0)	38±29				
Ki-67 index (%)[a]		1.042	[1.005–1.080]	0.025*	1.01	[0.963–1.058]	0.694
Mitotic count (10HPF)[a]		1.1	[1.059–1.145]	< 0.001**			
Extent of invasion							
Limited in pancreas	63	10 (15.9)	148±21	< 0.001**	1		
Extended to other organ	25	13 (52.0)	70±12		1.113	[0.332–3.726]	0.862
Angioinvasion							
Absent	58	7 (12.1)	170±19	< 0.001**	1		
Present	30	16 (53.3)	70±11		3.338	[1.128–9.8722]	0.029*
Perineural invasion							
Absent	73	16 (21.9)	133±18	0.005**	1		
Present	15	7 (46.7)	46±8		0.842	[0.210–3.384]	0.843
pT (AJCC 7th edn)							
1	32	2 (6.2)	192±16	< 0.001**			

	Univariate analysis				Multivariate analysis		
	n	Progression (%)	Mean ± SE (month)	*P* value	Hazard ratio (95% CI)		*P* value
2	31	8 (25.8)	94±11				
3	25	13 (52.0)	70±12				
pN							
0	80	19 (23.7)	129±18	0.002**	1		
1	8	5 (62.5)	36±11		3.097	[0.680–14.119]	0.144
pM							
0	81	18 (22.2)	128	0.003**	1		
1	7	5 (71.4)	59		2.029	[0.435–9.458]	0.368

[a] by Cox regression analysis, hazard ratio [95% confidence interval],

* $P < 0.05$,

** $P < 0.01$